IEEE Access
Multidisciplinary ⋮ Rapid Review ⋮ Open Access Journal

Received October 8, 2020, accepted October 30, 2020, date of publication November 4, 2020, date of current version November 16, 2020.

Digital Object Identifier 10.1109/ACCESS.2020.3035828

High Performance Supercapacitor Based on Laser Induced Graphene for Wearable Devices

MOHAMED R. R. ABDUL-AZIZ[1], A. HASSAN[1], AHMED A. R. ABDEL-ATY[1], MOHAMED R. SABER[1,2], RAMI GHANNAM[3], (Senior Member, IEEE), BADAWI ANIS[4], HADI HEIDARI[3], (Senior Member, IEEE), AND AHMED S. G. KHALIL[5,1]

[1]Environmental and Smart Technology Group, Faculty of Science, Fayoum University, Fayoum 63514, Egypt
[2]Department of Chemistry, Texas A&M University, College Station, TX 77842-3012, USA
[3]James Watt School of Engineering, University of Glasgow, Glasgow G12 8QQ, U.K.
[4]Spectroscopy Department, Physics Division, National Research Centre, Giza 12622, Egypt
[5]Materials Science & Engineering Department, School of Innovative Design Engineering, Egypt-Japan University of Science and Technology (E-JUST), Alexandria 21934, Egypt

Corresponding author: Ahmed S. G. Khalil (asg05@fayoum.edu.eg)

This work was supported in part by the Science and Technology Development Fund (STDF), Egypt (Project ID: 34947), and in part by the Engineering and Physical Sciences Research Council (EPSRC), U.K., under Grant EP/R511705/1. The work of Ahmed S. G. Khalil was supported by the Arab-German Young Academy for Sciences and Humanities (AGYA), Germany.

ABSTRACT To ensure maximum comfort for the wearer, electronic components that include energy harvesters need to be mechanically conformable. In this context, we demonstrate a versatile, cost-effective and efficient method for fabricating graphene supercapacitor electrodes using Laser Induced Graphene (LIG). A CO_2 laser beam instantly transforms the irradiated polyethersulfone polymer (PES) into a highly porous carbon structure. The LIG method was used to deposit graphene layers on graphite sheets to produce the supercapacitor electrodes. Graphene formation and morphology were examined and confirmed using several techniques including Scanning Electron Microscopy (SEM), Energy Dispersive X-ray (EDX) spectroscopy, Raman Spectroscopy and Fourier transform infrared spectroscopy (FTIR). Moreover, the electrochemical characterization was performed in different electrolytes (NaOH and KOH). At 5 mV s^{-1}, the LIG electrode achieved 165 mF cm^{-2} and 250 mF cm^{-2} in NaOH and KOH electrolytes, respectively. Consequently, we show that a wearable symmetric supercapacitor device with LIG electrodes achieved 98.5 mF cm^{-2} at 5 mV s^{-1} in KOH electrolyte. The device demonstrated an energy density of 11.3 μWh.cm^{-2} with power density of 0.33 mWcm^{-2} at 0.5 mA cm^{-2}. The retention of capacitance was 75% after 2000 cycles, with outstanding performance for the comparable graphene-based electrodes. These results further validate the use of LIG for developing flexible energy harvesters for wearable applications.

INDEX TERMS Laser induced graphene (LIG), graphene electrode, electrochemical double layer (EDLs), supercapacitor.

I. INTRODUCTION

Recently, the demand for novel energy storage devices has encouraged the development of novel materials for fabricating high-performance supercapacitors [1]. A supercapacitor is an effective energy storage technology that is lead-free, has ultrahigh power density, low internal resistance, and long cycle lifetime [2]. Energy storage in electric double-layer capacitors depends on the electrode surface ions absorption/desorption. Thus, ensuring higher electrode surface area is expected to significantly enhance the capacitance [3]. Whereas the pseudocapacitors store the energy via redox reactions on the electrodes surface [4]. Due to their large surface area, good electrical conductivity, porosity and excellent chemical stability, carbon-based materials are considered as promising candidates for energy storage applications [5]. Graphene as an interesting member of the carbon materials family has attracted great attention for supercapacitor applications due to its optimum physical and chemical properties, which includes its non-toxicity, controllability and versatility [6]–[10]. Graphene and reduced graphene oxide have been widely applied for supercapacitor applications [11]–[14].

The associate editor coordinating the review of this manuscript and approving it for publication was Abdul Halim Miah.

However, the fabrication process of reduced graphene oxide is complex and expensive [15].

Laser-induced graphene (LIG) is a newly developed method for the fabrication of advanced graphene-based devices [16]. LIG is produced using CO_2 infrared laser to directly write down on polymers. The polymer pyrolyzed due to induced localized heat, and therefore transformed into porous graphene structure [17]. The most common LIG substrates include polyether ether ketone [18], bakelite [19], [20], polyetherimide (PEI) [17], cloth [21] and wood [22]. Polyimide (PI) is widely used in LIG applications, [17], [23]–[25], owing to its thermal stability, mechanical properties, and excellent chemical resistance. However, the synthesis of PI is complex and tuning its porous structure is challenging [26]. Polyethersulfone (PES) and its derivatives have been widely used in different applications, such as membrane technology [27], electronics devices [28] and fuel cell [29]. In addition, LIG was realized on PES supports with the aim to enhance the antibacterial and antifouling properties [30]. The synthesis of PES is simple, and its porous properties can be tuned under certain optimized conditions. It has been found that the LIG-PES film shows lower sheet resistance (7 Ω/squ) [31], in the comparison to the one for LIG-PI films (15 Ω/squ) [17].

LIG structures consist of a few layers of graphene with three-dimensional configuration, leading to advantages such as ultrahigh surface area, excellent conductivity, and high porosity. Therefore, LIG has been touted to replace graphene in different applications such as electrocatalysis [32], microfluidic devices [33], sensors [34], and supercapacitors [35]–[37]. Recently, heteroatom and hybrid LIG films with enhanced properties have been reported in the literature [31], [37]. Generally, LIG electrodes fabricated from polymeric structures demonstrated lower capacitance due to limited specific surface area compared with other carbon-based materials, such as reduced graphene oxide [13]. Increasing the porosity of electrodes is expected to enhance the electrolyte accessibility, thus improving the capacitance as well as its corresponding power densities [13]. Due to the high porosity of the PES membranes, the laser treatment process can promote high electrochemical performance.

Herein, we present a novel alternative approach to fabricate LIG-based supercapacitor electrodes using a CO_2 laser. The graphene layers are directly formed on the graphite sheets. We also report the fabrication of a wearable supercapacitor with LIG electrodes and a KOH electrolyte. The fabrication process including the laser power, pulse duration as well as the membrane composition were optimized. The electrochemical supercapacitors electrode and device achieved a high capacitance and excellent stability in comparison to previously fabricated graphene-based supercapacitors.

II. EXPERIMENTAL WORK

A. PREPARATION OF PES MEMBRANES

PES sheets were synthesized using the phase separation method [27] and used as LIG substrate. Initially, pre-weighed 1.5 wt% of polyvinylpyrrolidone (PVP) was dissolved into 83.5 wt% N-Methyl-2-pyrrolidone (NMP) and stirred at 500 rpm for 60 minutes. Dried PES pellets (15 wt%) were then gradually added to the mixture. The solution was stirred at 500 rpm for 24 h to obtain a homogenous dope solution. The dope solution was cast on a clean glass plate using an automated casting machine. For all experiments, the membranes casting was carried out using a stainless-steel knife with a thickness of 200 μm and a speed of 5 mm/s. The sheet was immersed in a coagulation bath of deionized water at 21°C for ∼24 h to ensure complete precipitation. Finally, the sheet was dried in air and stored between two filter papers until use prior to the LIG process.

B. FABRICATION OF LIG ELECTRODE

All PES sheets were fixed flat on a graphite foil (0.4 mm thick, 99.8% (metals basis), Alfa Aesar) (1 × 1.5 cm^2) as a current collector, The graphite sheets were 1.5 × 1 cm^2, whereas the working electrode was deposited on 1 × 1 cm^2. Any residue membranes were peeled off from the substrate. CO_2 laser with 10.6 μm wavelength and 200 μm spot size, was used to convert the PES into graphene and deposit it on graphite sheet. In all experiments, the laser power was adjusted at 4.8 W, and the laser scan rate was set at ∼ 5 mm/s.

C. FABRICATION OF THE WEARABLE SUPERCAPACITOR

A symmetric 2-electrode supercapacitor was assembled using the two prepared identical LIG electrodes (1 cm × 1 cm). A filter paper (thickness 160 μm and pore size 20-25 μm) wetted with 6 M KOH aqueous electrolyte was used as a separator.

D. MATERIAL CHARACTERIZATION

The PES sheets and LIG electrodes were characterized using SEM to investigate the morphologies. Raman spectroscopy and Fourier transform infrared spectroscopy (FTIR) was performed to observe the surface functionalities and confirm the graphitization of polymer. A parameter analyzer (Keithley 4200-SCS) was used to characterize the resistivity of LIG electrodes.

E. ELECTROCHEMICAL CHARACTERIZATION

The electrochemical performance of LIG supercapacitor electrodes was tested in both 3-electrode and 2-electrode systems, with a platinum counter electrode and Ag/AgCl reference electrode. Different electrolytes were used (6M NaOH or 6M KOH). We used a similar characterization procedure reported in [38]. We carried out cyclic voltammetry (CV) measurements in a voltage range from −0.8 to 0.4 V at scan rates ranging from 5 to 500 mV s^{-1}. Similarly, Galvanostatic charge-discharge (GCD) experiments were performed at different current densities (0.5 to 10 mA cm^{-2}) and electrochemical impedance spectroscopy (EIS) measurements were carried out in the frequency range from 10 KHz to 100 mHz with 5 mV potential amplitude using an electrochemical workstation (CHI660E, CHI Instruments). The electrode was

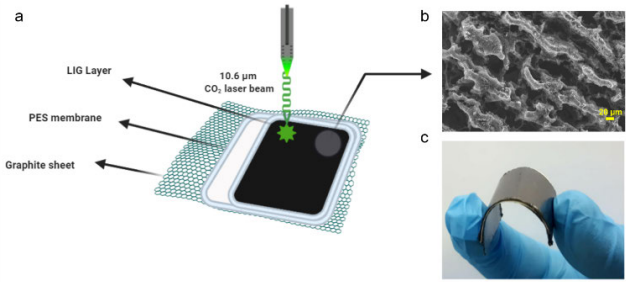

FIGURE 1. Fabrication of LIG film on graphite sheet.

placed in the electrolyte for 2 h before every measurement to guarantee sufficient wetting. Moreover, the CV measurement results were subsequently used for determining the specific capacitance (C_S, in $mFcm^{-2}$) using eq. 1 [17], [38].

$$Cs = \frac{\int IdV}{vS\Delta V} \tag{1}$$

where v is the scan rate (in Vs^{-1}), S is the total surface area of the electrode (in cm^{-2}), ΔV is the potential difference (V), and $\int$ I dV is the total area under the CV curve. Furthermore, C_S can be calculated using the GCD test using eq. 2 [39].

$$Cs = \frac{i\Delta t}{\Delta V} \tag{2}$$

where i is the current density (in mA cm^{-2}) and Δt is the discharge time (s). The fabricated device's energy density (E), in $\mu Whcm^{-2}$ of can subsequently be determined using:

$$E = \frac{Cs(\Delta V)^2}{2 \times 3600} \tag{3}$$

The power density (P), in $mWhcm^{-2}$ of the device, was calculated according to eq.4

$$P = \frac{3600 \times E}{\Delta t} \tag{4}$$

III. RESULTS AND DISCUSSION

A. FABRICATION AND CHARACTERIZATION OF LIG FILM

A schematic description of the LIG formation is shown in Fig. 1a. The PES sheets were converted into porous graphene using laser scribing. Fig.1b shows the SEM image of the lines induced by the laser beam. The photograph of the fabricated LIG supercapacitor is shown in Fig.1c.

SEM images of the top and cross-section of the PES and LIG films are shown in Fig. 2. The surface of PES has a relatively homogenous pore distribution (Fig. 2a). Once it's converted to LIG film, highly porous structure can be observed (Fig. 2c), which arises by removal of gaseous groups (sulfur and oxygen) from the PES matrix during the laser treatment [16]. At the microscale, the morphology of the LIG electrode is quite uniform with a relatively homogenous distribution of porosity. This porosity allows the electrolyte to penetrate the electrode, thereby increasing the overall efficiency of the supercapacitor device [44].

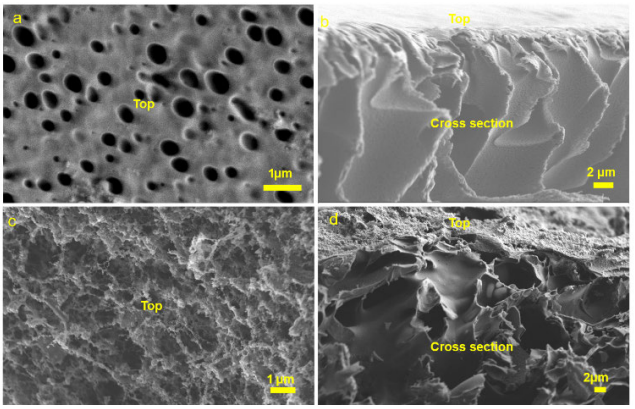

FIGURE 2. SEM images of top surface and cross section of PES membranes sheets (a, b) and LIG film (c, d).

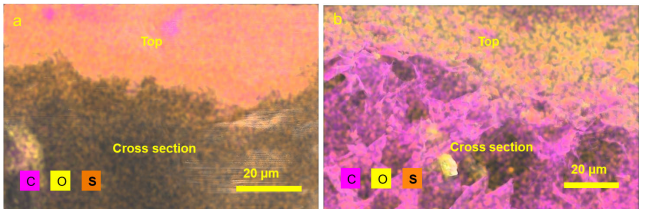

FIGURE 3. EDX mapping of cross-section (a) PES sheet (a) the LIG film.

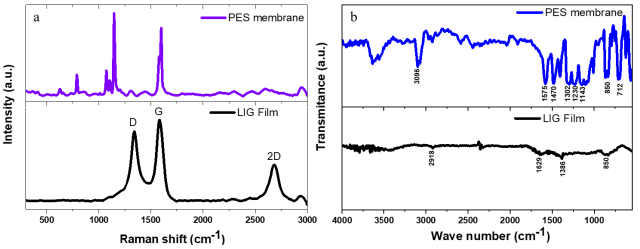

FIGURE 4. (a) Raman Spectra of PES and LIG films and (b) FTIR spectroscopy of PES and LIG films.

Cross-sectional SEM images of the PES and LIG films at the same magnification are shown in Fig. 2b, d. PES polymeric sheet has a dense skin layer with a finger-like structure. Whereas layered flakes observed in the LIG film can be attributed to successfully converting the PES film to porous graphene sheets. It can be observed that the cross-section porosity of PES and LIG is relatively low in comparison with the top surface. This could be due to the increase in the solvent exchange rate and the boost in the polymer concentration during the phase separation process, allowing for the construction of a dense skin layer [40]. This porosity is expected to enhance the capacitance performance in the device as electrolyte ions can easily pass through the porous structure leading to improved capacitance and electrode wettability.

The cross-section EDX mapping of PES and LIG sheets are shown in Fig. 3a,b. The PES sheet reveals the presence of carbon, oxygen, and sulfur (73%, 23.5% and 3.5%, respectively). The sharp increase of carbon content

versus oxygen and sulfur (93.6%, 6.11% and 0.29%) indicates a significant reduction of the PES film (ca. 95%) into graphene both on the surface and through the cross-section upon laser treatment (Fig. 3b). Furthermore, the high carbon content along LIG cross-section improved the LIG film conductivity which is expected to enhanced capacitance performance.

Raman spectra of PES sheet and LIG film (Fig. 4) clearly demonstrate the successful formation of the graphene oxide layer. The aromatic C–S and the aromatic ring chain of PES C–C peaks were observed. For the LIG film, the D-peak referred to the disordered structure of graphene, the G- peak indicated E_{2g} mode arises from the C-C bond, and 2D- peak originating from the second-order zone-boundary phonons of the LIG film were obtained [41].

FTIR was carried out on the PES and LIG films to confirm the graphitization (Fig. 4b). For PES, the peaks at 850 and 3096 cm^{-1} were due to the aromatic ring (C-H stretch). The C= C stretching appeared at peaks 1470 and 1575 cm^{-1}. The two peaks of the functional group sulfone (O = S = O stretching) were presented at 1143 and 1302 cm^{-1}. The peaks 1230 cm^{-1} and at 712 cm^{-1} may be attributed to C-S stretching [42]. For LIG films, no peaks related to functional groups (O = S = O and C-O-C) were shown. Furthermore, the stretching peaks C = C and C-H were reduced to small peaks. This may confirm the effective transformation of the PES into graphene by laser treatment.

The electrical resistivity was measured using parameter analyzer (Keithley 4200-SCS). The LIG electrode presented a sheet resistance of 5 Ω/squ, which is higher than the sheet resistance obtained for PI (15 Ω/squ) [17].

B. ELECTROCHEMICAL PERFORMANCE OF LIG ELECTRODES

The electrochemical characteristics of the LIG supercapacitor electrodes were obtained using the three electrodes configuration. The LIG electrode, platinum wire and Ag/AgCl were employed as working electrode, counter and as a reference electrode, respectively. Ag/AgCl reference electrode was calibrated with a standard calomel electrode before and after the experiment in saturated KCl [43]. The different electrolytes (6M NaOH and 6M KOH) were used to characterize the LIG electrode.

Fig. 5a presents the CV curves and GCD behavior of the LIG electrode. Fig. 5a present the CV curves of LIG in KOH and NaOH electrolytes at 20 mV s^{-1} scan rate. The CV curves are similar in performance for both electrolytes, which suggests the capacitance principally creates from electrical double-layer capacitance [3]. CVs can maintain rectangular shape for up to 300 mV s^{-1}. There are no redox peaks although their remnant small amount of pair redox functional groups (sulfur and oxygen) on LIG film [17]. Moreover, the performance of the LIG electrode was also performed by GCD curves for both electrolytes, as presented in Fig. 5b. The GCD curves retained nearly linear and symmetric charge-discharge profiles.

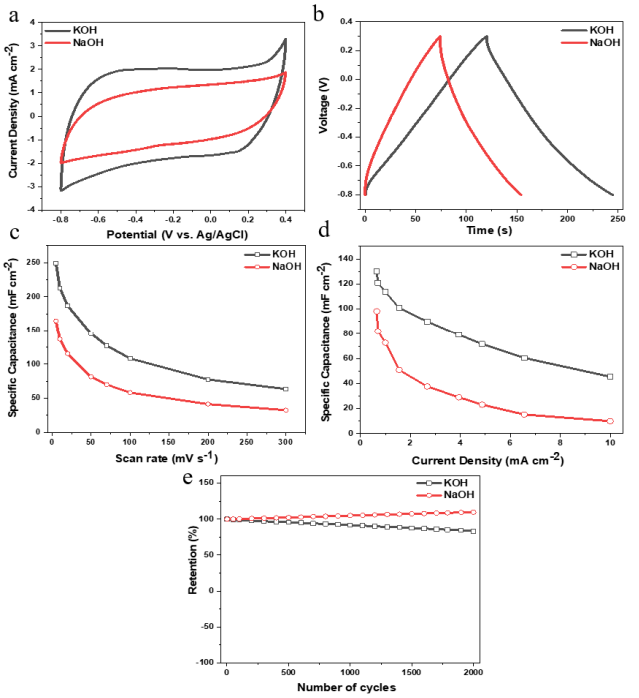

FIGURE 5. The electrochemical performance of LIG-SCs electrode in different electrolytes. (a) CV at 20mVs^{-1}, (b) GCD at 1 mAcm^{-2}, (c) specific capacitance of the LIG at different scan rate, (d) Specific capacitance of the LIG at different current densities and (e) cyclability of LIG electrode over 2000 cycles.

The specific capacitance of the LIG in the two electrolytes at scan rate in range 5 mVs^{-1} – 300 mVs^{-1} is shown in Fig. 5c. The specific capacitance gradually decreased from 165 mF cm^{-2} (∼165 Fg^{-1}) at 5 mVs^{-1} to 32 mFcm^{-2} at 300 mVs^{-1} for NaOH. Using KOH resulted in higher values of 250 mFcm^{-2} (∼250 Fg^{-1}) and 63 mFcm^{-2} at 5 mVs^{-1} and 300 mVs^{-1}. The dependence of specific capacitance on current density is shown in Fig. 5d. The capacitance gradually decreased from 98 mFcm^{-2} (∼98 Fg^{-1}) at 0.5 mAcm^{-2} to 10 mFcm^{-2} at 10 mAcm^{-2} for NaOH. The capacitance also decreased from 130mFcm^{-2} (∼130 Fg^{-1}) at 0.5mAcm^{-2} to 27 mFcm^{-2} at 10mAcm^{-2} for KOH. The higher performance for KOH is due to its lower hydration radius (3.31 Å) and higher ionic conductivity (73$cm^2\Omega^{-1}mol^{-1}$) in comparison to the Na+ ions, showing hydrated radius (3.58 Å) and 50 $cm^2\Omega^{-1}mol^{-1}$ conductivity [44]. In both cases, the observed specific capacitance is higher than the previously reported graphene-based supercapacitor (Table 1) [18], [20], [36], [45], [46]. Several parameters are attributed for enhancing the LIG supercapacitor performance including high surface area, excellent electrical conductivity, and good porosity with homogenous pore distribution overall the film, which could allow higher diffusion of K^+ and Na^+ ions [44]. The electrode has retained 91.5% and 83% of the initial capacitance in KOH with 100% columbic efficiency after 1000 and 2000 GCD cycles respectively (Fig 4e). Similarly, the NaOH electrolyte demonstrates much higher stability with ∼100% retention and ∼100 % columbic efficiency after 2000 GCD cycles.

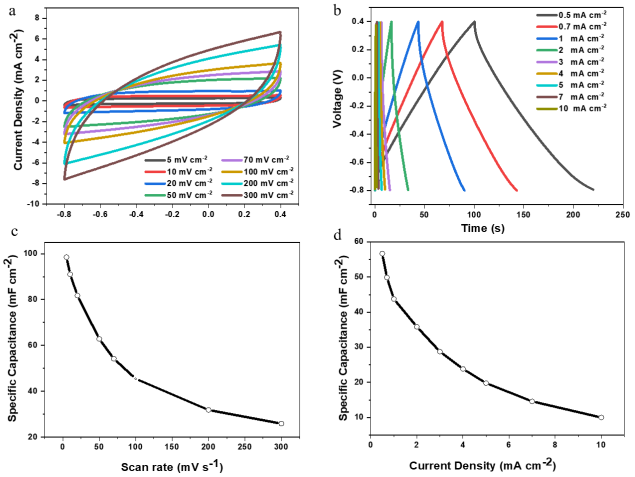

FIGURE 6. The electrochemical performance of LIG symmetric device in KOH. (a) CV curves at different scan rate, (b) GCD curves of LIG device at different current density, (c) specific capacitance at different scan rate and (d) specific capacitance at different current densities.

C. ELECTROCHEMICAL PERFORMANCE OF THE SYMMETRIC DEVICE

We evaluated the capacitance performance of symmetric LIG device in 6M KOH electrolyte. Fig. 6a presents the CV curves of LIG supercapacitor device at various scan rates. The quasi-rectangular CV curves were observed, suggesting the capacitor possessed excellent electrical double-layer capacitance behavior [3]. This behavior could be confirmed by stable triangle shape of the GCD at different current density (Fig. 6b). The data obtained from the GCD and CV measurements used to calculate the specific capacitance according to eq. 1 and 2. The specific capacitance obtained at different scan rate (Fig. 6c), showed a gradual decrease from 98.5 $mFcm^{-2}$ ($\sim$ 98.5 Fg^{-1}) at $5mVs^{-1}$ to 26 mF cm^{-2} at 300 mVs^{-1}. Fig. 6d reveals that the GCD specific capacitance can maintain up to a high current density of 10 $mAcm^{-2}$, indicating the capacitor exhibits excellent power density performance. At discharge current of 0.5 $mAcm^{-2}$, the specific capacitance was 56.6 $mFcm^{-2}$ and 9 $mFcm^{-2}$ at 10 $mAcm^{-2}$. The LIG device performance exhibited a high specific capacitance in comparison to previously reported graphene-based SCs (Table 1) [19], [47]–[50].

The Nyquist plot was fitted to equivalent circuit model Randles circuit [51] as shown in Fig. 7a, where R1 is the equivalent series resistance (ESR), R2 is the electrode electrolyte resistance, R3 is the resistance of leakage. Q1 is the double layer phase constant, W_0 is the Warburg, and Q2 is capacitance mass. In Fig. 7b Ragone plot presents the power density versus energy density calculated from GCD data. LIG supercapacitor reveals the highest energy density of 11.3, 8.75, 4, 2 μ $Whcm^{-2}$ with a maximum power density of 0.337, 0.67, 4.45, 9 $mWcm^{-2}$ at current density of 0.5, 1, 5, 10 $mAcm^{-2}$, respectively. This is in good agreement with previously reported graphene SCs [47], [49]. The LIG device maintained a stability of 83.6% and 75% after 1000 and 2000 GCD cycles, as can be seen from Fig. 7c. The stability

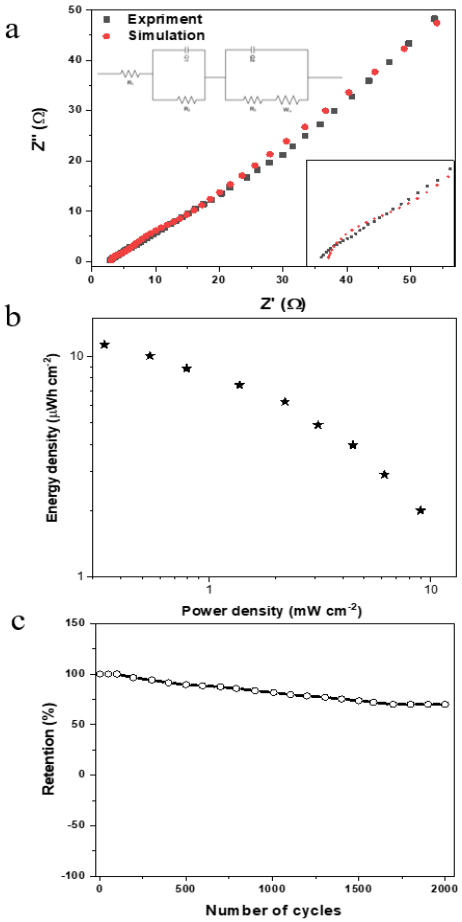

FIGURE 7. (a) Nyquist plot of LIG supercapacitor device for experimental and simulated data, (b) Ragone plot of LIG device, (c) cyclability of LIG device over 2000 cycle.

of the 2-electrode LIG device is relatively smaller than that of the 3-electrode system. This could be attributed to a higher ionic diffusion resulting from the separator, in addition to the distances between the two electrodes during the electrochemical test [52]. Moreover, the coulomb efficiency was 94% after 2000 GCD cycles.

Both devices were fabricated via LIG technique in this study using either the 3-electrode or the 2-electrode system. LIG in 3-electrode system in 6 M KOH exhibited much higher performance than in 6 M NaOH, including the high specific capacitance of 250 mF cm^{-2} at 5 mV s^{-1} and excellent cyclability of 91.5% after 1000 cycles. These results illustrated that the porous structure of the LIG electrode improved the wettability and electrical conductivity. Also, a 2-electrode symmetric supercapacitor based LIG presented a capacitance level of 98.5 $mFcm^{-2}$ at scan rate $5mVs^{-1}$, a high energy density of 11.3 μWh cm^{-2} (11.3 Wh Kg^{-1}) at 0.5 $mAcm^{-2}$, and excellent power density of 4.45 mW cm^{-2} (4453 W Kg^{-1}) at 5 $mAcm^{-2}$. These performances indicate that LIG is a promising as graphene-based electrode for supercapacitor applications. The result of both devices in comparison to previously reported LIG, laser reduced graphene (LrGO) and reduced graphene (rGO) electrodes shown in Table 1.

TABLE 1. Performance of graphene based 31 supercapacitors previously published in literature.

ELECTRODE MATERIAL	ELECTROLYTE	POTENTIAL WINDOW	MEASUREMENT	CAPACITANCE	REF
LIG electrode	1M Na_2SO_4	0.5 to -0.5	3-electrode	30 mF cm^{-2} at 3 mV s^{-1}	36
LIG electrode	1M Na_2SO_4	0 to -0.7	3-electrode	20.4 mF cm^{-2} at 10 mV s^{-1}	18
LIG electrode	1M Na_2SO_4	-0.1 to -1	3-electrode	1.9 mF cm^{-2} at 20 mV s^{-1}	20
LIG electrode	1M Na_2SO_4	0.5 to -0.5	2-electrode	18.5 mF cm^{-2} at 5 mV s^{-1}	19
LrGO electrode	1M H_2SO_4	0 to 0.8	2-electrode	95 mF cm^{-2} at 1 mA cm^{-2}	49
LrGO electrode	0.5M Na_2SO_4	0 to1	2-electrode	141 F g^{-1} at 1.04 A g^{-1}	48
LrGO electrode	1 M Na_2SO_4	0 to -0.6	2-electrode	185 F g^{-1} at 5 mV s^{-1}	47
rGO electrode	0.5 M NaOH	0.4 to -0.8	3-electrode	39.5 F g^{-1} at 5 A g^{-1}	46
rGO electrode	6 M KOH	0 to1	2-electrode	122.5 at 0.3 A g^{-1}	50
rGO electrode	6 M KOH	0.2 to -0.7	3-electrode	115 at 1 A g^{-1}	45
LIG electrode	6 M NaOH	0.4 to -0.8	3-electrode	165 mF cm^{-2} at 5 mV s^{-1} 98 mF cm^{-2} at 0.5 mA cm^{-2}	*This Work*
	6 M KOH		3-electrode	250 mF cm^{-2} at 5 mV s^{-1} 130mF cm^{-2} at 0.5 mA cm^{-2}	
	6 M KOH		2-electrode	98.5 mF cm^{-2} at 5 mV s^{-1} 56.6 mF cm^{-2} at 0.5 mA cm^{-2}	

IV. CONCLUSION

In this article, we demonstrated a simple and high throughput method for fabricating graphene-based supercapacitors. LIG was used to fabricate the supercapacitor electrode, where the ability to fabricating a high conductive and highly porous graphene layers were examined. Thus, leading to enhance the electrochemical behavior of LIG electrode either in three electrode or in two electrode systems. Besides, the direct deposit a graphene layer on graphite sheets and the electrochemical characterization have been reported for the first time. These advantages given the experimentally improved here present new methods to fabricate a graphene based materials for different applications such as electrocatalysis, sensors, microfluidic devices and energy storage

REFERENCES

[1] E. E. Miller, Y. Hua, and F. H. Tezel, "Materials for energy storage: Review of electrode materials and methods of increasing capacitance for supercapacitors," *J. Energy Storage*, vol. 20, pp. 30–40, Dec. 2018.
[2] A. K. Shukla, A. Banerjee, M. K. Ravikumar, and A. Jalajakshi, "Electrochemical capacitors: Technical challenges and prognosis for future markets," *Electrochim. Acta*, vol. 84, pp. 165–173, Dec. 2012.
[3] J. R. Miller, R. A. Outlaw, and B. C. Holloway, "Graphene double-layer capacitor with AC line-filtering performance," *Science*, vol. 329, no. 5999, pp. 1637–1639, Sep. 2010.
[4] Y. Gogotsi and R. M. Penner, "Energy storage in nanomaterials-capacitive, pseudocapacitive, or battery-like," Tech. Rep., 2018, pp. 2081–2083.
[5] F. Wang, X. Wu, X. Yuan, Z. Liu, Y. Zhang, L. Fu, Y. Zhu, Q. Zhou, Y. Wu, and W. Huang, "Latest advances in supercapacitors: From new electrode materials to novel device designs," *Chem. Soc. Rev.*, vol. 46, no. 22, pp. 6816–6854, 2017.
[6] A. K. Geim, "Graphene: Status and prospects," *Science*, vol. 324, no. 5934, pp. 1530–1534, Jun. 2009.
[7] Q. J. Le, M. Huang, T. Wang, X. Y. Liu, L. Sun, X. L. Guo, D. B. Jiang, J. Wang, F. Dong, and Y. X. Zhang, "Biotemplate derived three dimensional nitrogen doped graphene@ MnO_2 as bifunctional material for supercapacitor and oxygen reduction reaction catalyst," *J. Colloid Interface Sci.*, vol. 544, pp. 63–155, May 2019.
[8] J. Chen, C. Li, and G. Shi, "Graphene materials for electrochemical capacitors," *J. Phys. Chem. Lett.*, vol. 4, no. 8, pp. 1244–1253, 2013.
[9] M. F. El-Kady, Y. Shao, and R. B. Kaner, "Graphene for batteries, supercapacitors and beyond," *Nature Rev. Mater.*, vol. 1, no. 7, pp. 1–4, Jul. 2016.
[10] M. D. Stoller, S. Park, Y. Zhu, J. An, and R. S. Ruoff, "Graphene-based ultracapacitors," *Nano Lett.*, vol. 10, pp. 3498–3502, Oct. 2008.
[11] A. S. Mayorov, R. V. Gorbachev, S. V. Morozov, L. Britnell, R. Jalil, L. A. Ponomarenko, P. Blake, K. S. Novoselov, K. Watanabe, T. Taniguchi, and A. K. Geim, "Micrometer-scale ballistic transport in encapsulated graphene at room temperature," *Nano lett.*, vol. 11, no. 6, pp. 2396–2399, 2011.
[12] D. Aradilla, M. Delaunay, S. Sadki, J.-M. Gérard, and G. Bidan, "Vertically aligned graphene nanosheets on silicon using an ionic liquid electrolyte: Towards high performance on-chip micro-supercapacitors," *J. Mater. Chem. A*, vol. 3, no. 38, pp. 19254–19262, 2015.
[13] M. F. El-Kady, V. Strong, S. Dubin, and R. B. Kaner, "Laser scribing of high-performance and flexible graphene-based electrochemical capacitors," *Science*, vol. 335, no. 6074, pp. 1326–1330, Mar. 2012.
[14] M. F. Hossain, J. Yin, and J.-Y. Park, "Fabrication and characterization of reduced graphene oxide modified nickel hydroxide electrode for energy storage applications," *Jpn. J. Appl. Phys.*, vol. 53, no. 8S3, Aug. 2014, Art. no. 08NC02.
[15] Y. Zhu, S. Murali, W. Cai, X. Li, J. W. Suk, J. R. Potts, and R. S. Ruoff, "Graphene and graphene oxide: Synthesis, properties, and applications," *Adv. Mater.*, vol. 22, pp. 3906–3924, Sep. 2010.
[16] R. Ye, D. K. James, and J. M. Tour, "Laser-induced graphene: From discovery to translation," *Adv. Mater.*, vol. 31, no. 1, Jan. 2019, Art. no. 1803621.
[17] J. Lin, Z. Peng, Y. Liu, F. Ruiz-Zepeda, R. Ye, E. L. G. Samuel, M. J. Yacaman, B. I. Yakobson, and J. M. Tour, "Laser-induced porous graphene films from commercial polymers," *Nature Commun.*, vol. 5, no. 1, pp. 1–8, Dec. 2014.
[18] C. Zhu, D. Zhao, K. Wang, X. Dong, W. Duan, F. Wang, M. Gao, and G. Zhang, "Direct laser writing of graphene films from a polyether ether ketone precursor," *J. Mater. Sci.*, vol. 54, no. 5, pp. 4192–4201, Mar. 2019.
[19] F. Wang, X. Mei, K. Wang, X. Dong, M. Gao, Z. Zhai, J. Lv, C. Zhu, W. Duan, and W. Wang, "Rapid and low-cost laser synthesis of hierarchically porous graphene materials as high-performance electrodes for supercapacitors," *J. Mater. Sci.*, vol. 54, no. 7, pp. 5658–5670, Apr. 2019.
[20] F. Wang, W. Duan, K. Wang, X. Dong, M. Gao, Z. Zhai, X. Mei, J. Lv, W. Wang, and C. Zhu, "Graphitized hierarchically porous carbon nanosheets derived from bakelite induced by high-repetition picosecond laser," *Appl. Surf. Sci.*, vol. 450, pp. 155–163, Aug. 2018.
[21] Y. Chyan, R. Ye, Y. Li, S. P. Singh, C. J. Arnusch, and J. M. Tour, "Laser-induced graphene by multiple lasing: Toward electronics on cloth, paper, and food," *ACS Nano*, vol. 13, pp. 2176–2183, Feb. 2018.
[22] R. Ye, Y. Chyan, J. Zhang, Y. Li, X. Han, C. Kittrell, and J. M. Tour, "Laser-induced graphene formation on wood," *Adv. Mater.*, vol. 29, Oct. 2017, Art. no. 1702211.
[23] K. Rathinam, S. P. Singh, Y. Li, R. Kasher, J. M. Tour, and C. J. Arnusch, "Polyimide derived laser-induced graphene as adsorbent for cationic and anionic dyes," *Carbon*, vol. 124, pp. 515–524, Nov. 2017.
[24] A. Tiliakos, C. Ceaus, S. M. Iordache, E. Vasile, and I. Stamatin, "Morphic transitions of nanocarbons via laser pyrolysis of polyimide films," *J. Anal. Appl. Pyrol.*, vol. 121, pp. 275–286, Sep. 2016.
[25] S. Naveed, T. Malik, M. Muneer, and M. A. Mohammad, "A laser scribed graphene oxide and polyimide hybrid strain sensor," *Key Eng. Mater.*, vol. 778, pp. 169–174, Sep. 2018.
[26] D.-J. Liaw, K.-L. Wang, Y.-C. Huang, K.-R. Lee, J.-Y. Lai, and C.-S. Ha, "Advanced polyimide materials: Syntheses, physical properties and applications," *Prog. Polym. Sci.*, vol. 37, no. 7, pp. 907–974, Jul. 2012.
[27] I. M. A. ElSherbiny, R. Ghannam, A. S. G. Khalil, and M. Ulbricht, "Isotropic macroporous polyethersulfone membranes as competitive supports for high performance polyamide desalination membranes," *J. Membrane Sci.*, vol. 493, pp. 782–793, Nov. 2015.
[28] S. von Kraemer, M. Puchner, P. Jannasch, A. Lundblad, and G. Lindbergh, "Gas diffusion electrodes and membrane electrode assemblies based on a sulfonated polysulfone for high-temperature PEMFC," *J. Electrochem. Soc.*, vol. 153, no. 11, 2006, Art. no. A2077.

[29] L. Karlsson, "Polysulfone ionomers for proton-conducting fuel cell membranes: Sulfoalkylated polysulfones," *J. Membrane Sci.*, vol. 230, nos. 1–2, pp. 61–70, Feb. 2004.
[30] S. P. Singh, Y. Li, J. Zhang, J. M. Tour, and C. J. Arnusch, "Sulfur-doped laser-induced porous graphene derived from polysulfone-class polymers and membranes," *ACS Nano*, vol. 12, no. 1, pp. 289–297, Jan. 2018.
[31] M. R. R. Abdul-Aziz, S. A. Mohassieb, N. A. Eltresy, M. M. K. Yousef, B. Anis, S. O. Abdellatif, and A. S. G. Khalil, "Enhancing the performance of polygon monopole antenna using graphene/TMDCs heterostructures," *IEEE Trans. Nanotechnol.*, vol. 19, pp. 269–273, 2020.
[32] J. Zhang, C. Zhang, J. Sha, H. Fei, Y. Li, and J. M. Tour, "Efficient water-splitting electrodes based on laser-induced graphene," *ACS Appl. Mater. Interface*, vol. 9, no. 32, pp. 26840–26847, Aug. 2017.
[33] M. A. Khan, I. R. Hristovski, G. Marinaro, and J. Kosel, "Magnetic composite hydrodynamic pump with laser-induced graphene electrodes," *IEEE Trans. Magn.*, vol. 53, no. 11, pp. 1–4, Nov. 2017.
[34] L.-Q. Tao, H. Tian, Y. Liu, Z.-Y. Ju, Y. Pang, Y.-Q. Chen, D.-Y. Wang, X.-G. Tian, J.-C. Yan, N.-Q. Deng, Y. Yang, and T.-L. Ren, "An intelligent artificial throat with sound-sensing ability based on laser induced graphene," *Nature Commun.*, vol. 8, no. 1, pp. 1–8, Apr. 2017.
[35] Z. Peng, J. Lin, R. Ye, E. L. G. Samuel, and J. M. Tour, "Flexible and stackable laser-induced graphene supercapacitors," *ACS Appl. Mater. Interface*, vol. 7, no. 5, pp. 3414–3419, Feb. 2015.
[36] A. Lamberti, M. Serrapede, G. Ferraro, M. Fontana, F. Perrucci, S. Bianco, A. Chiolerio, and S. Bocchini, "All-SPEEK flexible supercapacitor exploiting laser-induced graphenization," *2D Mater.*, vol. 4, no. 3, Jul. 2017, Art. no. 035012.
[37] L. Li, J. Zhang, Z. Peng, Y. Li, C. Gao, Y. Ji, R. Ye, N. D. Kim, Q. Zhong, Y. Yang, and H. Fei, "High-performance pseudocapacitive microsupercapacitors from laser-induced graphene," *Adv Mater.*, vol. 28, no. 5, pp. 838–845, 2016.
[38] B. A. Ali, A. M. A. Omar, A. S. G. Khalil, and N. K. Allam, "Untapped potential of polymorph MoS2: Tuned cationic intercalation for high-performance symmetric supercapacitors," *ACS Appl. Mater. Interface*, vol. 11, no. 37, pp. 33955–33965, Sep. 2019.
[39] J. Lin, C. Zhang, Z. Yan, Y. Zhu, Z. Peng, R. H. Hauge, D. Natelson, and J. M. Tour, "3-dimensional graphene carbon nanotube carpet-based microsupercapacitors with high electrochemical performance," *Nano Lett.*, vol. 13, no. 1, pp. 72–78, Jan. 2013.
[40] X. Tan and D. Rodrigue, "A review on porous polymeric membrane preparation. Part I: Production techniques with polysulfone and poly (vinylidene fluoride)," *Polymers*, vol. 11, no. 7, p. 1160, Jul. 2019.
[41] B. Anis, A. Abouelsayed, W. El Hotaby, A. M. Sawy, and A. S. G. Khalil, "Tuning the plasmon resonance and work function of laser-scribed chemically doped graphene," *Carbon*, vol. 120, pp. 44–53, Aug. 2017.
[42] F. F. Ghiggi, L. D. Pollo, N. S. M. Cardozo, and I. C. Tessaro, "Preparation and characterization of polyethersulfone/N-phthaloyl-chitosan ultrafiltration membrane with antifouling property," *Eur. Polym. J.*, vol. 92, pp. 61–70, Jul. 2017.
[43] M. H. Yun, J. W. Yeon, J. Hwang, C. S. Hong, and K. Song, "A calibration technique for an Ag/AgCl reference electrode utilizing the relationship between the electrical conductivity and the KCl concentration of the internal electrolyte," *J. App. Electrochem.*, vol. 39, no. 12, p. 2587, 2009.
[44] B. Pal, S. Yang, S. Ramesh, V. Thangadurai, and R. Jose, "Electrolyte selection for supercapacitive devices: A critical review," *Nanosc. Adv.*, vol. 1, no. 10, pp. 3807–3835, 2019.
[45] P. Luo and Y. Lin, "Further thermal reduction of reduced graphene oxide aerogel with excellent rate performance for supercapacitors," *Appl. Sci.*, vol. 9, no. 11, p. 2188, May 2019.
[46] M. Talebi, P. Asen, S. Shahrokhian, and M. M. Ahadian, "Polyphosphate-reduced graphene oxide on ni foam as a binder free electrode for fabrication of high performance supercapacitor," *Electrochim. Acta*, vol. 296, pp. 130–141, Feb. 2019.
[47] Q. Liu, Q. Shi, H. Wang, Q. Zhang, and Y. Li, "Laser irradiated self-supporting and flexible 3-dimentional graphene-based film electrode with promising electrochemical properties," *RSC Adv.*, vol. 5, no. 58, pp. 47074–47079, 2015.
[48] D. Yang and C. Bock, "Laser reduced graphene for supercapacitor applications," *J. Power Sources*, vol. 337, pp. 73–81, Jan. 2017.
[49] T. X. Tran, H. Choi, C. H. Che, J. H. Sul, I. G. Kim, S.-M. Lee, J.-H. Kim, and J. B. In, "Laser-induced reduction of graphene oxide by intensity-modulated line beam for supercapacitor applications," *ACS Appl. Mater. Interface*, vol. 10, no. 46, pp. 39777–39784, Nov. 2018.
[50] G. Luo, H. Huang, Z. Cheng, C. Lei, X. Wu, S. Tang, and Y. Du, "Synthesis of graphene on ni foam with enhanced capacitive performance by embedding PS spacers," *Mater. Technol.*, vol. 34, no. 9, pp. 499–505, Jul. 2019.
[51] R. S. Hastak, P. Sivaraman, D. D. Potphode, K. Shashidhara, and A. B. Samui, "All solid supercapacitor based on activated carbon and poly [2,5-benzimidazole] for high temperature application," *Electrochim. Acta*, vol. 59, pp. 296–303, Jan. 2012.
[52] J. Liang, A. K. Mondal, D.-W. Wang, and F. Iacopi, "Graphene-based planar microsupercapacitors: Recent advances and future challenges," *Adv. Mater. Technol.*, vol. 4, no. 1, Jan. 2019, Art. no. 1800200.

MOHAMED R. R. ABDUL-AZIZ received the B.Sc. degree from the Faculty of Science, Fayoum University, Egypt, in 2018. Since 2018, he has been a Research Assistant with the Environmental and Smart Technology Group, Fayoum University. His research interests are on carbon nanomaterials, hybrid graphene structure, Laser-induced graphene, energy storage, and energy harvesting applications.

A. HASSAN received the Ph.D. degree in solid-state physics from the Dresden University of Technology, Germany, in 2014. He is currently a Lecturer with the Faculty of Science, Fayoum University, Egypt. His research interests are in carbon nanomaterials, superconducting materials, laser-induced graphene for energy storage applications, and synthesis and magnetic properties of new materials for energy applications.

AHMED A. R. ABDEL-ATY received the B.Sc. degree from the Faculty of Science, Fayoum University, Egypt, in 2017. Since 2017, he has been a Research Assistant with the Environmental and Smart Technology Group, Fayoum University. His research interests include functional polymeric and nanohybrid materials, including synthetic membranes and membrane-based technologies for water purification.

MOHAMED R. SABER received the Ph.D. degree in chemistry from Texas A&M University, College Station, TX, USA, in 2013. Since 2015, he has been an Assistant Professor with the Chemistry Department, Fayoum University, and a Visiting Professor at Texas A&M University, lecturing nanoscience, general and inorganic chemistry, and molecular spectroscopy. He is leading research on functional nanomaterials for energy, water, and biomedical applications; fabrication and testing of biosensors; photophysical properties of nanomaterials; and synthesis and magneto-structural studies of magnetic materials. He has participated in establishing the center of environmental and smart technology (CEST), including securing funds, purchase and installation of several high-end instruments (CVD, AFM, SEM, Time resolved PL, PPMS). He has been organizing and conducting training workshops on nanomaterials synthesis and applications, water desalination, and solar energy.

RAMI GHANNAM (Senior Member, IEEE) received the B.Eng. degree in electronic engineering from King's College, the DIC and M.Sc. degrees from Imperial College London, and the Ph.D. degree from the University of Cambridge, in 2007. He held previous industrial positions at Nortel Networks and IBM Research GmbH. He is currently a Lecturer (Assistant Professor) in electronic and nanoscale engineering with the University of Glasgow. His research interests are in energy harvesters and engineering education. He is a Senior Fellow of Glasgow's RET scheme and serves as Scotland's Regional Chair of the IEEE Education Society. He was awarded the Siemens Prize from King's College.

BADAWI ANIS received the Ph.D. degree in the spectroscopy of carbon nanomaterials from Augsburg University, Germany, in 2013. He is currently holding a postdoctoral position with Augsburg University from 2013 to 2014. He is currently an Associate Professor of Spectroscopy with the National Research Centre, Cairo. His research focuses on terahertz spectroscopy of carbon nanomaterials, single-chirality nanotubes, Laser-induced graphene for energy storage applications, as well as carbon nanomaterials for water purification.

HADI HEIDARI (Senior Member, IEEE) is currently an Associate Professor (Senior Lecturer) and the Head of the Microelectronics Lab (meLAB), School of Engineering, University of Glasgow, U.K. He has authored over 150 publications in peer-reviewed journals, i.e., the IEEE Solid-State Circuits Journal, IEEE Transactions on Circuits and Systems I and IEEE Transactions Electron Devices, and in international conferences. He has been a recipient of a number of awards, including the IEEE CASS Scholarship (NGCAS'17 Conference), the Silk Road Award from the Solid-State Circuits Conference (ISSCC'16), the Best Paper Award from the IEEE ISCAS'14 Conference, Gold Leaf Award from the IEEE PRIME'14 Conference and Rewards for Excellence prize from the University of Glasgow (2018). He involves in organizing committees of the IEEE PRIME'15, SENSORS'16, '17, IEEE NGCAS'17, BioCAS'18, ISCAS'20,'23 conferences and chairing three special sessions at ISCAS'16,'17,'18. He is a member of the IEEE Circuits and Systems Society Board of Governors (BoG), and the IEEE Sensors Council Administrative Committee (AdCom). He is the General Chair of the IEEE International Conference on Electronics Circuits and Systems (ICECS) 2020. He is an Editor for the *Elsevier Microelectronics Journal* and the Lead Guest Editor for four journal special issues.

AHMED S. G. KHALIL received the B.Sc. and M.Sc. degrees in physics from Cairo University, in 1999 and 2003, respectively, and the Ph.D. degree in physics and materials science from Max Planck Institute, Germany, in 2008. He was a Postdoctoral Associate (2008–2010) with the University of Duisburg-Essen, Germany, and a visiting scientist at IBM Research Labs, Zurich, Switzerland (2010–2011), and the University of California at Berkley, Berkley, CA, USA (2013). He is the founder and group leader of the Environmental and Smart Technology Group (ESTG). His scientific research has been published in highly ranked journals, such as *Advanced Materials*, *Journal of American Chemical Society*, *Journal of Materials Chemistry*, *Desalination*, *Carbon and Journal of Membrane Science*. His research interests expand into different areas, including water desalination, printed electronics, and solar energy. Over the last six years, he has succeeded to attract more than Euro 6 Million from national and international funding organizations for his research and teaching activities at Fayoum University and the Egypt-Japan University of Science and Technology. These activities have been done in close collaboration with more than 50 academic and industrial partners from the USA, Europe, Asia, and the Arab world. Since 2016, he has been an elected member of the Arab German Academy of Science and Humanities (AGYA) in Germany. He is currently an Associate Professor of Materials Science at the Faculty of Engineering, Egypt-Japan University of Science and Technology (E-JUST), Egypt, and on sabbatical leave from his position at the Faculty of Science, Fayoum University.